Effects of cyclic carbonates as additives to γ-butyrolactone electrolytes for rechargeable lithium cells

Shin-chi Kinoshita[a], Minoru Kotato[a], Yuichi Sakata[a], Makoto Ue[a], Yuu Watanabe[b], Hideyuki Morimoto[b], Shin-ichi Tobishima[b],*

[a] Mitsubishi Chemical Group Science and Technology Research Center, Inc., 8-3-1 Chuo, Ami, Inashiki, Ibaraki 300-0332, Japan
[b] Department of Chemistry, Faculty of Engineering, Gunma University, 1-5-1 Tenjincho, Kiryu, Gunma 376-8515, Japan

ABSTRACT

γ-Butyrolactone (GBL) has a high boiling point, a low freezing point, a high flashing point, a high dielectric constant and a low viscosity. GBL is a very preferable solvent for lithium ion batteries. However, GBL readily undergoes reductive decomposition on the surface of the negative electrodes, and it forms a solid electrolyte interphase (SEI) with a large resistance. It is causing deterioration of battery performances. In this work, effects of cyclic carbonates as additives to GBL electrolytes were investigated. As these carbonates, ethylene carbonate (EC), propylene carbonate (PC), vinylene carbonate (VC), vinylethylene carbonate (VEC), and phenylethylene carbonate (PhEC) were investigated using $LiCoO_2$/graphite cells. The effects of these additives were evaluated from the viewpoints of improvement of the battery performance and suppression of the reductive decomposition of GBL. VC, VEC and PhEC were effective to suppress the excess reductive decomposition of GBL. Battery performances were improved and the following results were obtained from the electrochemical measurements of $LiCoO_2$/graphite cells with GBL-based electrolytes. Residual capacity was high in the order of VEC > VC > PhEC. Rate capability was high in the order of PhEC > VC > VEC. These additives have advantages and disadvantages. By optimizing electrolyte formulation, the performances of Li-ion batteries using GBL-based electrolytes will be improved further.

© 2008 Elsevier B.V. All rights reserved.

1. Introduction

Many of organic solvents used for electrolyte solutions of lithium ion cells are cyclic and linear carbonates. Table 1 shows physical properties of these solvents [1–4]. Mixed solvents of ethylene carbonate (EC) and linear carbonates such as dimethyl carbonate (DMC), ethylmethyl carbonate (EMC), and diethyl carbonate (DEC) are often used to obtain high conductivity and tolerance for the oxidation at high charge voltage (4.2 V) of lithium ion cells. However, these liner carbonates have low boiling points below 150 °C and low flashing points below 30 °C (Table 1). These are disadvantageous from the safety aspect.

On the other hand, γ-butyrolactone (GBL) has a high boiling point of 204 °C, a low freezing point of −44 °C, a high flashing point of 101 °C, a high dielectric constant of 42 and a low viscosity of 1.7 mPa s. GBL is a very preferable solvent for lithium ion batteries [5,6]. However, GBL readily undergoes reductive decomposition on the surface of the negative electrodes, and it forms a solid electrolyte interphase (SEI) with a large resistance [7]. It is causing deterioration of battery performances. Aurbach has demonstrated that reductive GBL decomposition mainly produces lithium butylate and cyclic alkoxy-β-keto ester lithium salt [7]. It is considered that the excess formation of these compounds cause a large resistance of the cells.

In order to improve the battery performance, many electrolyte additives have been proposed [8]. For example, vinylene carbonate (VC) was developed by SAFT in the first place [9]. Aurbach et al. proposed that VC forms polymeric surface species, which enhance SEI stability [10]. However, these additives were mainly investigated to carbonate-based electrolytes. Little is known about their suitability to GBL electrolytes.

In this work, effects of cyclic carbonates as additives to GBL electrolytes were investigated. As these carbonates, EC, propylene carbonate (PC), VC, vinylethylene carbonate (VEC) [11,12], and phenylethylene carbonate (PhEC) [13] were investigated. Chemical structure of these carbonates is shown in Fig. 1. We evaluated the effects of these additives from the viewpoints of improvement of the battery performance and suppression of the reductive decomposition of GBL.

* Corresponding author. Tel.: +81 277 30 1382; fax: +81 277 30 1380.
E-mail address: tobi@chem-bio.gunma-u.ac.jp (S.-i. Tobishima).

Table 1
Physical properties of organic solvents used in lithium ion batteries

	Boiling point (°C)	Freezing point (°C)	Flashing point (°C)	Dielectric constant at 25 °C	Viscosity at 25 °C (mPa^{-1} s^{-1})
Ethylene carbonate (EC)	244	37	143	90	1.9[a]
Dimethyl carbonate (DMC)	90	3	18	3.1	0.59
Ethyl methyl carbonate (EMC)	108	−55	23	2.9	0.65
Diethyl carbonate (DEC)	127	−43	25	2.8	0.75
γ-Butyrolactone (GBL)	204	−44	101	42	1.7

[a] 40 °C.
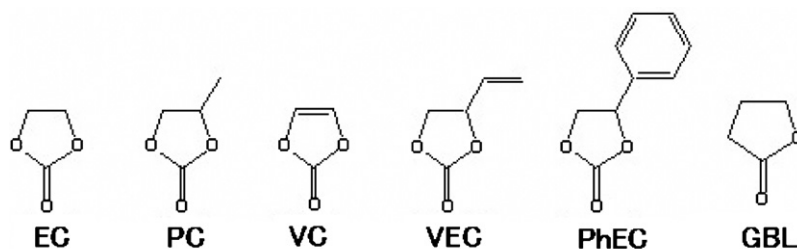
Fig. 1. Chemical structure of solvents.

2. Experimental

2.1. Electrolyte solutions

1 M (mole L^{-1}) LiBF$_4$ solution in GBL was used as the base electrolyte. Five compounds were used as additives. These are EC, PC, VC, VEC and PhEC. 5 wt% of VC and equimolar amounts of other additives were added into LiBF$_4$/GBL. 1 M LiBF$_4$/EC–EMC (volume mixing ratio = 30:70) was used as reference electrolyte.

2.2. Electrochemical measurements

To evaluate the reduction behavior of the electrolyte solutions, 2032-coin type cells (20 mm in diameter, 3.2 mm in thickness) using graphite/Li were used. The following battery performances were evaluated with 2032 coin type cells using LiCoO$_2$/graphite having a capacity of approximately 3.2 mAh; charge–discharge performance at first cycle, rate capability, storage test at 60 °C for a week, and charge–discharge cycle performance. These 2032 coin type cells have 23 mg (0.23 × 10^{-3} mole) LiCoO$_2$ and 10.5 mg (0.145 × 10^{-3} mole of C$_6$) graphite.

2032 type coin cells fabricated cells as previously mentioned were charged to 4.2 V at 0.2 C rate followed by a constant voltage charging to a cut-off current of 0.02 C rate (constant current–constant voltage (CC–CV) charging), and impedance measurement applied to these cells. And these cells were discharged to 3.0 V at 0.2 C rate. Similar charge and discharge cycles were performed with several discharge rate (0.2 C → 0.5 C → 1 C). And then, fully charged state (0.2 C–CC–CV charged state) cells were stored at 60 °C for a week. After storage test, first discharge capacity was determined as residual capacity. And rate capabilities were measured by the same method mentioned above.

2.3. Analysis methods

The evolved gas in the cell was analyzed by A Hewlett-Packard 6890 series gas chromatograph.

The components of the surface film on the graphite anode after a charge and discharge cycle were characterized by Fourier transform infrared spectroscopy (FT-IR) (Nicolet Magna 560) equipped with a TGS detector. Spectra were obtained using a resolution of 4 cm^{-1} and averaged over 64 scans. The measurement was carried out by the ATR method. The surface film was rinsed with highly purified DMC (battery grade, Mitsubishi Chemical Corporation).

X-ray photoelectron spectroscopy (XPS) (ULVAC-PHI5700ci) was used to obtain information about the elementary chemical state for the surface film. Monochromatic Al K radiation (1486.6 eV), which operated at a power of 350 W (14 kV), was applied as the X-ray source. All XPS measurements were done in the sample after a charge and discharge cycle. The surface film was rinsed with highly purified DMC (battery grade, Mitsubishi Chemical Corporation).

The impedance spectra were measured with impedance analyzer (SI 1280B Electrochemical Measurement Unit, Solartron Analytical, UK). The amplitude of the AC voltage was 5 mV. The impedance measurement was performed in a frequency range from 20 kHz to 10 mHz, and started from high frequency toward low frequency.

3. Results and discussion

3.1. Reduction behavior of electrolyte solutions

Reduction behavior of the electrolyte solutions was examined using graphite/Li coin cells. Fig. 2 shows the first discharge curves of graphite/Li cells at 0.1 C rate. The reduction potential of various solvents on graphite were estimated from this figure. When discharge of Li/graphite cells started, cell voltage sharply dropped from open circuit voltage (OCV) around 3 V to voltages of 0.2–1.5 V with medium voltage slope and with capacities of around 20 mAh g^{-1} based on carbon weight. Then, discharge voltage curves show the slow low voltage decrease region below 0.2 V with capacities of around 350 mAh g^{-1}. These low voltage regions correspond to the intercalation of lithium ions into the graphite layer. The high voltage regions of 0.2–1.5 V correspond to the electrochemical reduction of electrolyte solutions by lithium. This reaction produces surface film on the carbon electrode, which is generally called a solid electrolyte interface (SEI) [7]. Lithium ions can pass through this film and prevent further reaction between the electrolyte and lithium. This reaction leads to the irreversible capacity between the first charge and discharge. In this work, the voltages at the start of high voltage regions were determined as reduction potential (Ered) values of electrolyte solutions. Table 2 shows the Ered values measured and the calculation results of LUMO (lowest unoccupied molecular orbital) energy based on the reported calculation method [14].
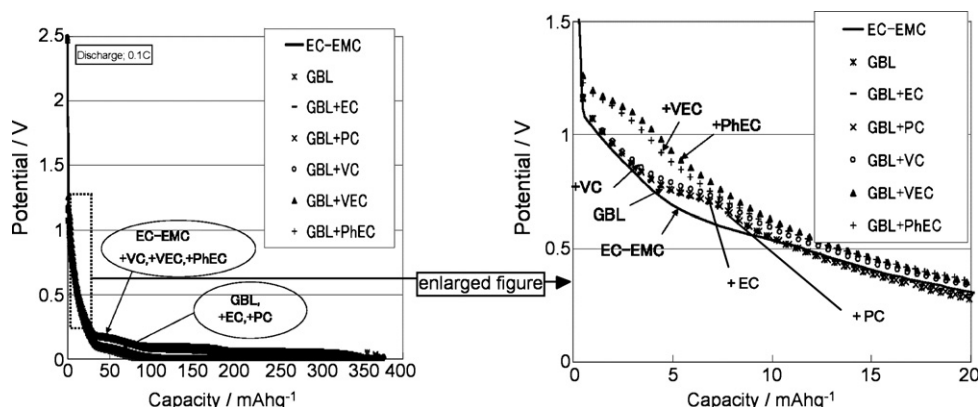
Fig. 2. First discharge curves of graphite/Li cells.

Table 2
Reduction potential (Ered) and LUMO energy of solvents

	Ered (V) vs. Li/Li⁺	LUMO energy (eV)
EC	1.07	5.612
PC	1.08	5.749
GBL	1.15	5.162
VC	1.17	4.453
VEC	1.23	3.945
PhEC	1.27	3.293

Reduction potential values tend to increase with a decrease in LUMO energy.

1.0 M LiBF$_4$/GBL electrolyte indicated higher reduction potential than that of 1.0 M LiBF$_4$/EC–EMC electrolyte. In the presence of additives, reduction potential was high in the order of PhEC (1.27 V vs. Li/Li⁺) > VEC (1.23 V) ≫ VC (1.17 V) ∼ GBL (1.15 V) ≫ PC (1.08 V) ∼ EC (1.07 V) > EC–EMC (1.04 V).

3.2. Electrochemical performance of LiCoO$_2$/graphite cells with GBL-based electrolytes

Battery performance was evaluated using LiCoO$_2$/graphite cells with various electrolyte solutions. Fig. 3 shows the first charge–discharge curves of these LiCoO$_2$/graphite cells. These cells were charged to 4.2 V at 0.2 C rate followed by a constant voltage charging to a cut-off current of 0.02 C rate. This is called as CC–CV charging. Then, cells were discharged to 3.0 V at 0.2 C rate. Charge–discharge capacity was calculated based on the weight of LiCoO$_2$. In the presence of VC, VEC and PhEC, the discharge capacity increased and discharge voltage was higher than those of the cells
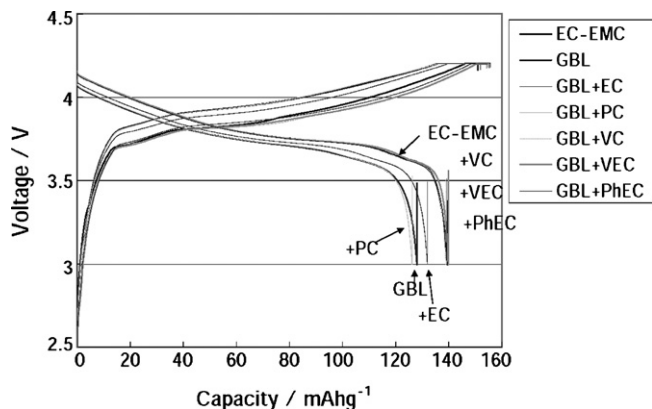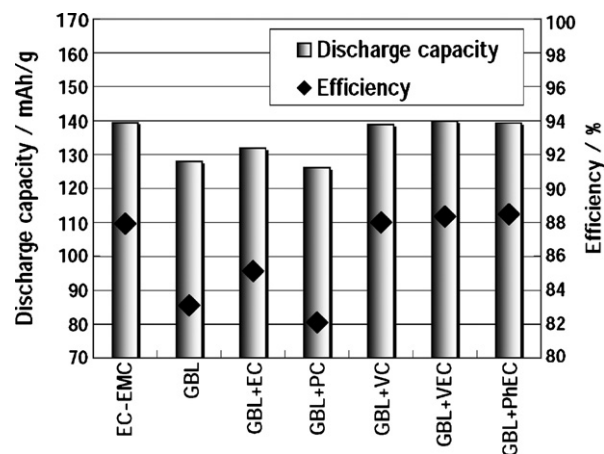

Fig. 4. Discharge capacity and charge–discharge efficiency.

having GBL electrolyte without additives. These effects of addition of EC and PC to GBL were very small.

Fig. 4 shows discharge capacity values and charge–discharge efficiencies obtained from the charge–discharge cycle tests mentioned above. In the presence of VC, VEC and PhEC, discharge capacity and efficiency were improved, compared with those of GBL alone. These discharge capacity and efficiency values of GBL+VC, VEC and PhEC were almost same as that of EC–EMC electrolyte. Fig. 5 shows the relation between charge and discharge cycling efficiencies at the first cycle obtained from Li/graphite cells (efficiency (Li/C)) and graphite/LiCoO$_2$ cells (efficiency (Co/C)). Effi-
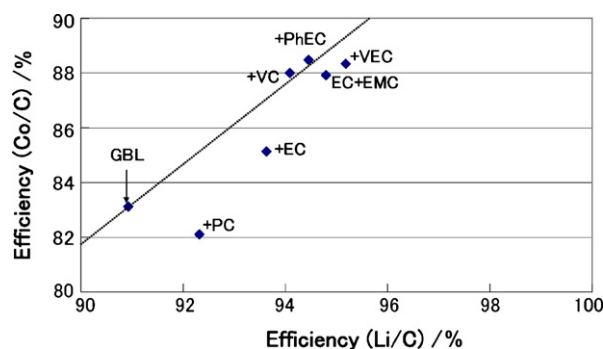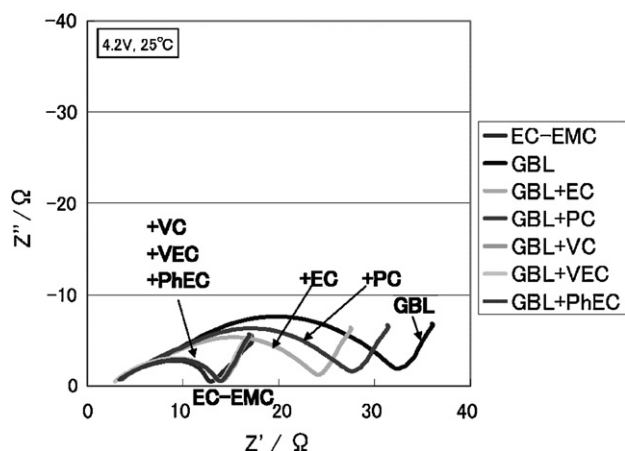

Fig. 3. First charge–discharge curves of LiCoO$_2$/graphite cells.

Fig. 5. Relation between charge and discharge cycling efficiencies at the first cycle obtained from Li/graphite cells (efficiency (Li/C)) and graphite/LiCoO$_2$ cells (efficiency (Co/C)).

Fig. 6. Impedance spectra at first charged state of LiCoO$_2$/graphite cells.

ciencies of graphite/LiCoO$_2$ cells tend to increase with an increase in efficiencies of Li/graphite cells. Therefore, cycling efficiency of graphite/LiCoO$_2$ cells is determined mainly by the SEI formation of carbon anodes.

Fig. 6 shows the impedance spectra of graphite/LiCoO$_2$ cells at first charged state. These cells were charged to 4.2 V at 0.2 C rate followed by a constant voltage charging to a cut-off current of 0.02 C rate. GBL electrolyte without additive showed very large resistance. In the presence of VC, VEC and PhEC, resistances were very low. This means that VC, VEC and PhEC produced an effective SEI, and this SEI suppressed the excessive decomposition of GBL.

Fig. 7 shows discharge capacities of graphite/LiCoO$_2$ cells at various discharge rates of 0.2 C, 0.5 C and 1 C. In the presence of VC, VEC and PhEC, discharge capacity increased and these capacities were almost same as that of EC–EMC electrolyte.

Fig. 8 shows the discharge capacities after storage at 60 °C for a week. In the presence of VC, VEC and PhEC, residual capacities after storage were relatively high. Residual capacity (capacity after self-discharge) is high in the order of VEC > VC > PhEC. Especially, VEC showed higher residual capacity. After measuring the residual capacity, cells were charged by standard CC–CV charging. Then, cells were discharged again, and recovery capacities were measured. Recovery discharge capacity at 1 C rate of VEC was little bit lower than those of VC and PhEC. Rate capability obtained by charging after storage is high in the order of PhEC > VC > VEC.

It is considered that, the SEI derived from VEC has high thermal stability but its interfacial resistance is large. The discharge
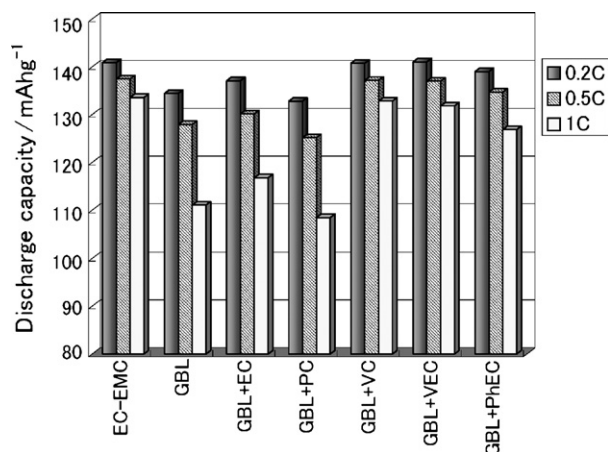
capacities of GBL electrolytes with various additives were relatively lower than that of EC–EMC electrolyte. It is necessary to improve further.

Charge–discharge cycle performances of graphite/LiCoO$_2$ cells with various electrolytes were examined. Fig. 9 shows the discharge capacity at 0.2 C rate as a function of the cycle number. GBL electrolyte containing of VC, VEC and PhEC showed good cycle performance. This cycle performance was better than EC–EMC.

3.3. Properties of surface film on anodes and reactivity of additives

In order to obtain the information of SEI and reaction of additives, we performed the analysis of evolved gas and SEI formed on graphite surface after first cycle. Fig. 10 shows the result of evolved gas analysis. Hydrogen, ethylene, carbon dioxide and carbon monooxide were detected in the EC–EMC electrolyte. Ethylene gas is formed by reduction of EC as shown in Eq. (1). On the other hand, in GBL electrolyte, detected gas was mainly a hydrogen gas. In the presence of VEC, butadiene gas was detected. Butadiene gas was formed by reduction of VEC in the same way as EC. At contrast, the presence of EC and PC in GBL electrolyte, the amounts of ethylene and propylene gas were very small. These results also indicate that VEC is more reactive than GBL, and GBL is more reactive than EC and PC on graphite surface.

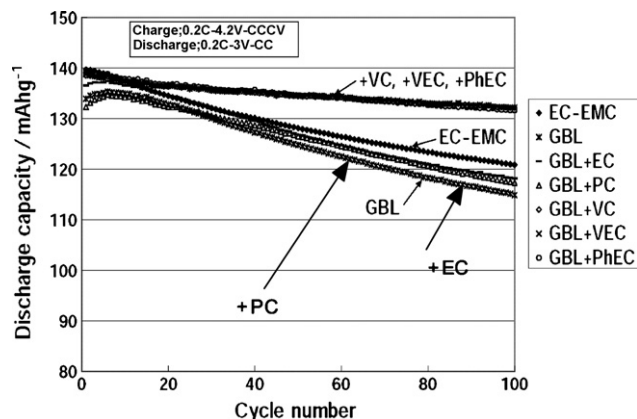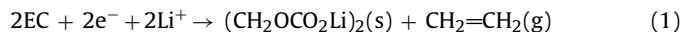$$2EC + 2e^- + 2Li^+ \rightarrow (CH_2OCO_2Li)_2(s) + CH_2{=}CH_2(g) \qquad (1)$$

Fig. 8. Discharge capacities of LiCoO$_2$/graphite cells after storage at 60 °C for a week.

Fig. 7. Discharge capacities at various discharge rates of LiCoO$_2$/graphite cells.

Fig. 9. Charge–discharge cycle performance of LiCoO$_2$/graphite cells.
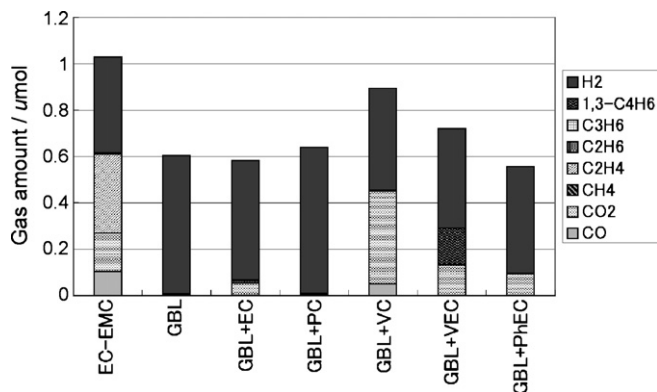
Fig. 10. Evolved gas analysis of LiCoO₂/graphite cells.

Table 3
Obtained effects of cyclic carbonate

	Reduction potential (V) vs. Li/Li⁺	Suppression of GBL decomposition	Possibility existence of polymeric materials
EC	1.07	Not effective	Low
PC	1.08	Not effective	Low
GBL	1.15	–	Low
VC	1.17	Effective	High
VEC	1.23	Very effective	High
PhEC	1.27	Very effective	Low

Fig. 11 shows the IR spectra of SEIs. The distinct peak appeared at $1580\,cm^{-1}$. This peak corresponds to the lithium carboxylate unit derived from decomposition compounds of GBL [7]. Reductive GBL decomposition is reported to mainly produce lithium butylate and cyclic alkoxy-β-keto ester lithium salt as shown in Fig. 12 [7]. The spectra of authentic samples of lithium acetate and GBL electrolyte were shown in Fig. 10. In the presence of VC, VEC, and PhEC, this peak intensity decreased. Peak intensity was high in the order of $GBL \gg VC > VEC$, PhEC. This means that VEC and PhEC are very

effective to suppress the decomposition of GBL. And this order was consistent with that of battery performance at first cycle shown in Fig. 9.

Fig. 13 shows the XPS spectra of SEI. This peak also corresponds to the decomposition compound of GBL, lithium acetate. In the presence of VC, VEC and PhEC, these peak intensities were decreased. This result was also consistent with that of IR measurement. Furthermore, in the presence of VC and VEC, additional peaks were detected at this peak position. So, we synthesized poly VC and poly VEC by polymerization of VC and VEC, respectively, as authentic sample [15]. Fig. 14 shows XPS spectra of polymer sample and SEI. These spectra are very similar. It is considered that these polymeric materials are probably formed on the surface of graphite.
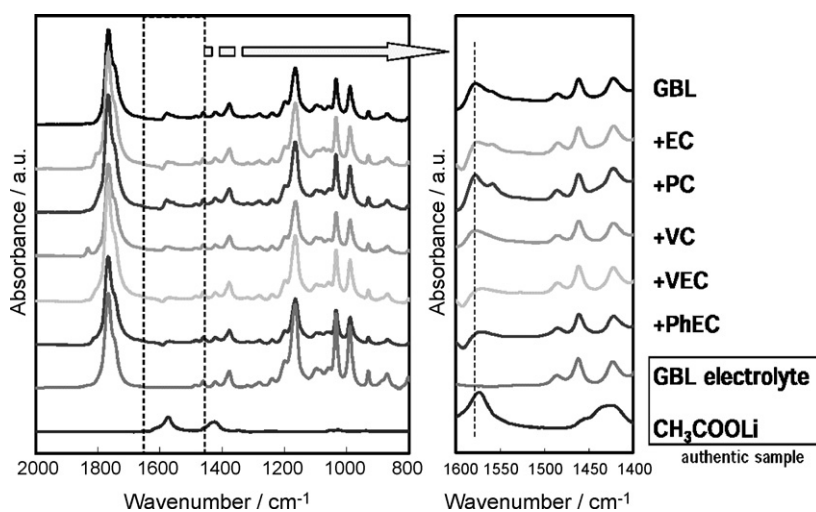

Fig. 11. IR spectra of SEI on graphite anodes of LiCoO₂/graphite cells.
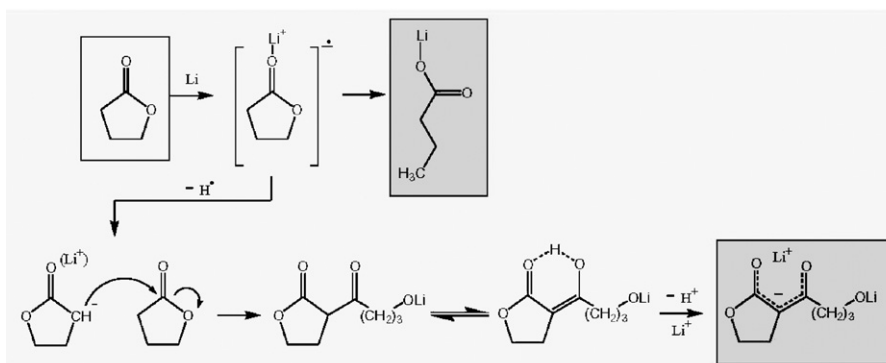

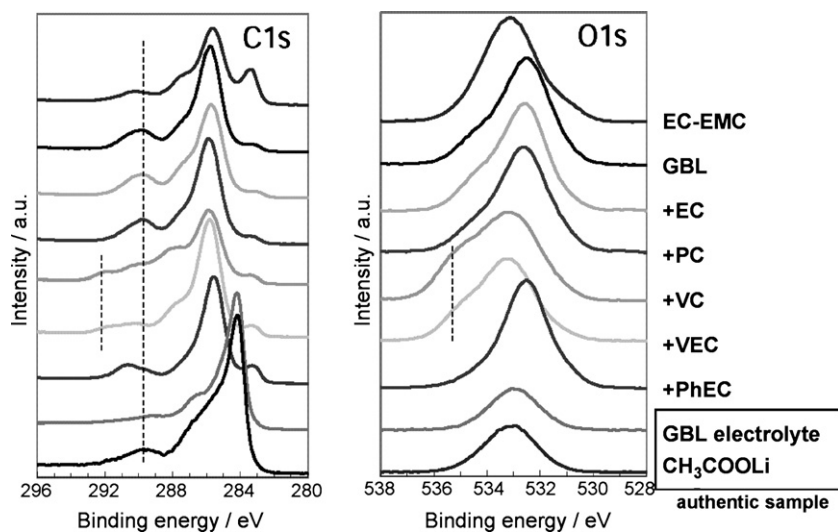**Fig. 12.** Reductive decomposition of GBL.

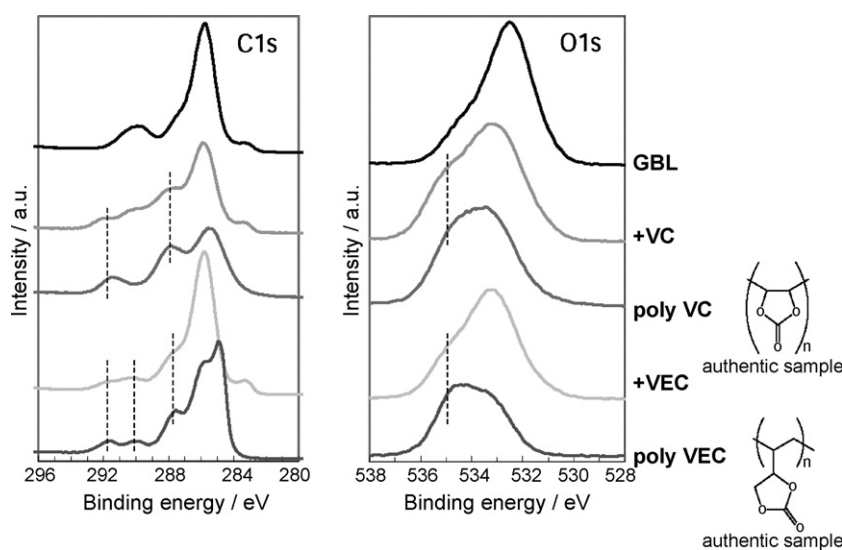Fig. 13. XPS spectra of SEI on graphite anodes of LiCoO$_2$/graphite cells.

Fig. 14. XPS spectra of SEI on graphite anodes of LiCoO$_2$/graphite cells, and XPS spectra of GBL with poly VC and poly VEC.

Table 3 summarizes the obtained effects of cyclic carbonate. VEC and PhEC were very effective to suppress the decomposition of GBL. Because, these compounds indicated higher reduction potentials. VC and VEC have a possibility to form polymeric SEI. Therefore, it showed high residual capacity. As for VEC, at least two reaction paths were considered. One is polymerization path. Another is elimination of butadiene gas.

4. Conclusion

In this work, effects of cyclic carbonates as additives to GBL electrolytes were investigated using LiCoO$_2$/graphite cells. VC, VEC and PhEC were effective to suppress the excess reductive decomposition of GBL. Battery performances were improved and the following results were obtained from the electrochemical measurements of LiCoO$_2$/graphite cells with GBL-based electrolytes. Residual capacity was high in the order of VEC > VC > PhEC. Rate capability was high in the order of PhEC > VC > VEC. These additives have advantages and disadvantages. By optimizing electrolyte formulation, the performances of Li-ion batteries using GBL-based electrolytes will be improved further.

References

[1] J.O. Besenhard (Ed.), Handbook of Battery Materials, Wiley–VCH, Weinheim, 1998.
[2] J.A. Riddick, W.B. Burger, Organic Solvents, 3rd ed., Wiley–Interscience, New York, 1970.
[3] T. Asakura (Ed.), Handbook of Organic Solvents, Kodansha, Japan, 1983 (in Japanese).
[4] G. Pistoia, M. De Rossi, B. Scrosati, J. Electrochem. Soc. 117 (1970) 500.
[5] N. Takami, T. Ohsaki, H. Hasebe, M. Yamamoto, J. Electrochem. Soc. 149 (2002) A9.
[6] A. Chagnes, B. Carre, P. Williman, R. Dedryvere, D. Gonbeau, D. Lemordart, J. Electrochem. Soc. 150 (2003) A1255.
[7] D. Aurbach, J. Electrochem. Soc. 136 (1989) 1606.
[8] M. Ue, Extended Abstracts of the Battery and Fuel Cell Materials Symposium, Gratz, Austria, 2004, p. 53.
[9] B. Simon, J.P. Boeuve, US Patent 5,626,981 (1997).
[10] D. Aurbach, K. Gamoisky, B. Maarkovsku, Y. Gofer, M. Schmidt, U. Heider, Electrochim. Acta 47 (2002) 1423.
[11] M. Kotato, T. Fujii, N. Shima, H. Suzuki, WO 00/79632 (2000).
[12] Y. Hu, W. Kong, H. Li, X. Huang, L. Chen, Electrochem. Commun. 6 (2004) 126.
[13] H. Suzuki, T. Sato, M. Kotato, H. Ota, H. Sato, US Patent 6,664,008 (2003).
[14] K. Tasaki, K. Kanda, T. Kobayashi, S. Nakamura, M. Ue, J. Electrochem. Soc. 153 (2006) A2192.
[15] Japanese Patent Application, Tokkai-223842 (1994).